Separation Science and Technology
Publication details, including instructions for authors and subscription information:
http://www.informaworld.com/smpp/title~content=t713708471

Monitoring of the Isotachophoretic Separation of Two Components with an Array Detector

Wolfgang Thormann[a]; Dieter Arn[b]; Ernst Schumacher[b]
[a] BIOPHYSICS TECHNOLOGY LABORATORY, UNIVERSITY OF ARIZONA, TUCSON, ARIZONA [b] INSTITUTE FOR INORGANIC CHEMISTRY UNIVERSITY OF BERN, BERN, SWITZERLAND

To cite this Article Thormann, Wolfgang , Arn, Dieter and Schumacher, Ernst(1984) 'Monitoring of the Isotachophoretic Separation of Two Components with an Array Detector', Separation Science and Technology, 19: 13, 995 — 1011
To link to this Article: DOI: 10.1080/01496398408058343
URL: http://dx.doi.org/10.1080/01496398408058343

SEPARATION SCIENCE AND TECHNOLOGY, 19(13-15), pp. 995-1011, 1984-85

Monitoring of the Isotachophoretic Separation of Two Components with an Array Detector

WOLFGANG THORMANN*

BIOPHYSICS TECHNOLOGY LABORATORY
UNIVERSITY OF ARIZONA
TUCSON, ARIZONA 85721

DIETER ARN and ERNST SCHUMACHER

INSTITUTE FOR INORGANIC CHEMISTRY
UNIVERSITY OF BERN
BERN, SWITZERLAND

Abstract

The introduction of an array detector along an isotachophoretic capillary allows monitoring of the separation process and the attainment of the steady-state zones, fully controlled by a microprocessor system. An apparatus where the potential gradient is measured at 255 equidistant positions along the separation space has been constructed. A description of this device is presented together with data showing the evolution of an isotachophoretic two-zone pattern.

INTRODUCTION

In isotachophoresis (ITP), sample components separate according to the moving boundary principle by forming consecutive zones with homogeneous concentrations. This system reaches a steady state in which each sample zone moves with constant velocity, hence the name isotachophoresis. The zone length is proportional to the amount of sample constituent. The beginning and the end of a zone are marked by a steady-

*To whom correspondence should be addressed at Chemical and Physical Sciences, Deakin University, Victoria, 3217, Australia.

 0149-6395/84/1913-0995$3.50/0

state electric field gradient as well as by a sudden change of other physical properties (*1–8*).

The ITP apparatus of Everaerts et al. (*2*) and Boček et al. (*3, 9*), as well as all commercially available analytical ITP instruments, have only one universal detector. Its location is at the end of the separation column. The usefulness of this mode of operation is severely limited because no information about the dynamics of a separation can be obtained in a single experiment. Using just one detector, it cannot be determined if steady state has been attained before the zone structure moves across the detector. Such a determination would require the repetition of each experiment with a different amount of sample and comparison of the results. By having many equidistant detectors along the column (*5, 6*) or by scanning the separation trough repeatedly with a moving detector (*10*), transient and steady-state zone distributions can be observed. When measuring a general physical property, the temporal development of each zone boundary can be monitored, including the vanishing of mixed zones. This gives a computer interpretable criterion of the steady state, which is a mandatory condition for automation.

A capillary-type apparatus with a multichannel detection device, permitting almost simultaneous measurements of the electric field at 255 positions along the separation trough, was constructed at the University of Bern, Switzerland (*5, 6*). In this article we wish to present the construction of the separation cell with the array detector together with a constant volume sample inlet system first developed by Ryser (*11*). Data showing the evolution of the separation of two components are given and compared to theoretical predictions made by a model based on migration only. Experiments are presented to illustrate the effect of a leading electrolyte cascade on the enhancement of the sample load of the separation column.

ASSEMBLY OF THE APPARATUS WITH AN ARRAY DETECTOR

Figure 1 shows an overall schematic of the apparatus with the array detector. A rectangular separation trough (TK), about $170 \times 0.7 \times 0.4$ mm, is connected to the sample inlet system (ES_1) and to the compartments with the driving electrodes (E_1, E_2). Both electrode reservoirs provide a virtually infinite supply of the electrode solutions and are hydrostatically separated from the separation trough by dialysis membranes (Me) which are good conductors for the ions. The leading electrolyte is in the right electrode vessel; the displacing electrolyte in the left. The capillary is rinsed simultaneously with both electrolytes from the reservoirs (V) and (L) by the

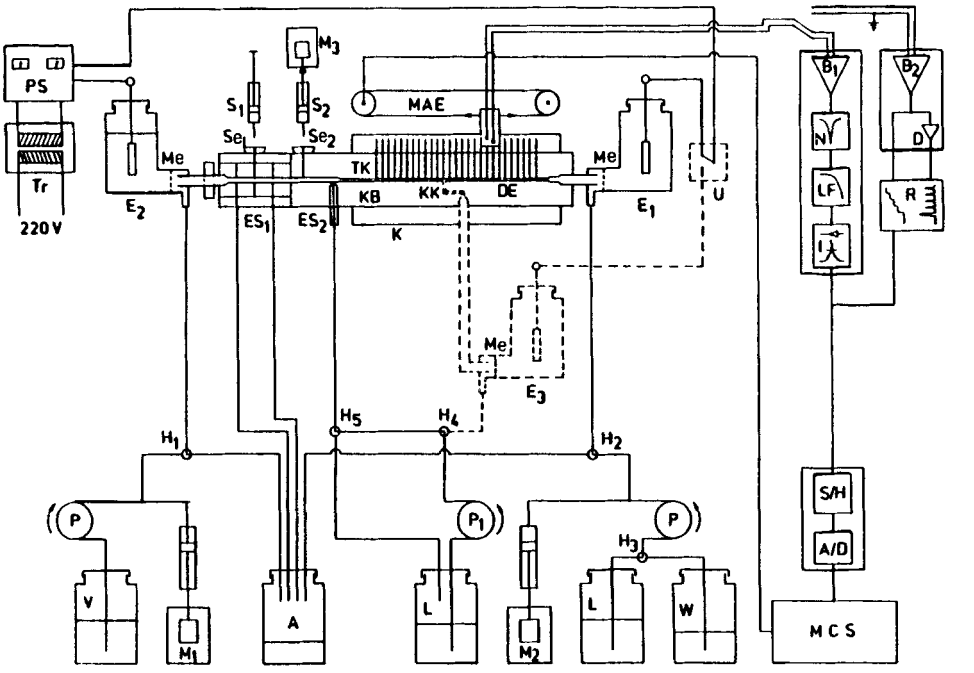

FIG. 1. Overall schematic of the isotachophoretic apparatus with an array detector. A) waste container; A/D) analog to digital converter; B_1, B_2) high impedance buffer; D) differentiator; DE) detection electrodes; E_1, E_2, E_3) Pt electrode vessels; ES_1) sample inlet system; ES_2) cascade electrolyte inlet; H_1-H_5) 3-way stopcocks with 90° channel; I) isolation amplifier; K) aluminum slab; KB) Plexiglass block; KK) channel coupling site; L) leading electrolyte; L') cascade leading electrolyte; LF) low pass filter; M_1, M_2) piston pumps for flow and counterflow; M_3) piston pump for continuous sampling; MAE) mechanical scanning device; MCS) microcomputer system; Me) ion permeable membranes; N) 50 Hz notch filter; P) 2-channel peristaltic pump; P_1) peristaltic pump for leading electrolyte cascade; PS) high voltage constant current power supply; R) 2-channel recorder; S_1, S_2) sample syringes; S/H) sample and hold amplifier; Se_1, Se_2) silicone septum; TK) separation trough; Tr) transformer with primary/secondary isolation > 20 kV; U) switch; V) displacing electrolyte; W) flushing reservoir.

two channel peristaltic pump (P) through the valve block (ES_1) into the waste flask (A). Then the sample is injected in excess by the syringe (S_1) through the septum (Se_1). The high voltage, current stabilized power supply (PS) operates through a transformer (T) which has a secondary output for more than 20 kV isolated from the primary and from ground. Appropriate detection electronics with high impedance input (B_1, B_2), a mechanical scanning device (MAE), and the microcomputer system (MCS) for control and data treatment complete the apparatus.

This instrument can be operated with a leading electrolyte cascade (*8, 12*). The leading electrolyte with a higher concentration (L') is introduced by a peristaltic pump (P_1) through a special inlet system (ES_2) or by a syringe through a septum (Se_2). Furthermore, the principle of column coupling (*13*) can be used. For that purpose the third electrode compartment (E_3) is connected to the coupling site (KK). Motor-driven piston pumps (M_1, M_2) are used for hydrodynamic displacement of the separation pattern as well as for the continuous sampling technique (M_3) (*14*).

The Separation Cell

The central functional unit of the system is the separation cell, consisting of 4 main parts, as shown in Fig. 2. It comprises a block of Plexiglas (KB) with valves and fittings, a silicone rubber gasket (D), an electrode-bearing glass plate (DE), and an aluminum plate (K). These parts are bolted together with eight screws and connected to the electrode vessels (E_1, E_2). The separation trough (32) consists of a rectangular main part between points (31) and (33) and two small cylindrical sections with a diameter of 1 mm (from 29 to 31 and 33 to 34, respectively). The dimension of the rectangular part is defined by the silicone gasket (D). Typically we choose a height of 0.5 mm and a channel width of 0.8 mm. Note that the whole separation trough is divided into two sections, a sensorless precolumn between (29) and (31) and the part with the multichannel detector. By varying the size of the precolumn and/or by using various silicone gaskets (D), the total volume of the separation space can easily be changed. The aluminum plate (K) is cooled by recirculation of fluid from an open thermostat.

The complete assembly of the sample inlet system is illustrated in Fig. 2. The valve block has a central cylindrical channel which is the continuation of the separation trough. Its sections (1a, 1b) allow the opening of three slits by turning the screw (4) counterclockwise. If the peristaltic pump (P) is now started and the stopcocks (H) are in the right position, the two electrolyte solutions enter the block from right and left. They flow out again through slits A and C, respectively, as shown schematically in Fig. 3(a). Slit B is connected to the sample injection port. After rinsing/filling with electrolyte, the sample is injected in excess. As illustrated in Fig. 3(b), the excess flows away through slits A and C, thus forming a sharp boundary with the two electrolytes. If screw (4) is now turned clockwise, the slits close, forming the initial pattern of boundaries which enclose a sample volume of about 7 μL, as indicated in Fig. 3(c).

The construction includes the following parts: Within the thick-walled

cylindrical metacrylate shell (5), which is part of the Plexiglas block (KB), three precisely machined sections (1a–1b) from polyethylene terephthalate or Teflon form the three slits between the cylindrical projections (1d) and their female counterpart on the next section. They are opened or closed by relaxing or applying pressure on the whole package exerted by screw (4) and counteracted by silicone O-rings (2). The three sections (1a, 1b) have drill holes with a fine channel connecting to the central channel in the device. This is the outlet or inlet for electrolytes when the slits are open. Screw (9b) with a one-sided flanged Teflon tube inset (9a) and a short piece of silicone tubing (9c) on the other side makes the connector for the input and output of the device. Through a threaded hole (15) in the shell (5), the assembly (9) is screwed tightly into the block valve. The piece of silicone tubing is thereby pressed into the drill hole of a valve section which guarantees a sealed connection.

The syringe injection port consists of a needle guide (17) and a silicone septum (18). The dead volume is very small. About 15 μL of sample solution has to be introduced in order to rinse the inlet port properly. Only about 7 μL are used for the analysis. This volume does not depend on the amount injected but is uniquely determined by the constant volume between the slits A and C (Fig. 3). Thus it is very easily reproduced. The sample injection port can also be connected directly (without septum) to a third channel of the peristaltic pump (P) which establishes the initial electrolyte arrangement in one step (Fig. 3d). Notice, however, that this requires the availability of larger volumes of sample solution. The additional septum inlet (21) at position (30) permits the injection of components with a syringe. This allows the performance of experiments with high sample loads using a leading electrolyte cascade. A higher concentration of the leading electrolyte is introduced into the sensorless section of the trough after the filling procedure with leading and displacing electrolyte is completed, but prior to the sample injection. This technique enhances the total amount of a sample component to be separated in a given column as described in Refs. *8* and *12*. The septum mounting at location (34) can be used for the withdrawal of single zones by a syringe.

The Array Detector

The impact of modern technology has lead to the miniaturization of integrated circuitry. In particular, etching processes allow the production of fine structures on an unharmed, solid substrate. We investigated chemical etching together with a photoresist. This method is widely used for the

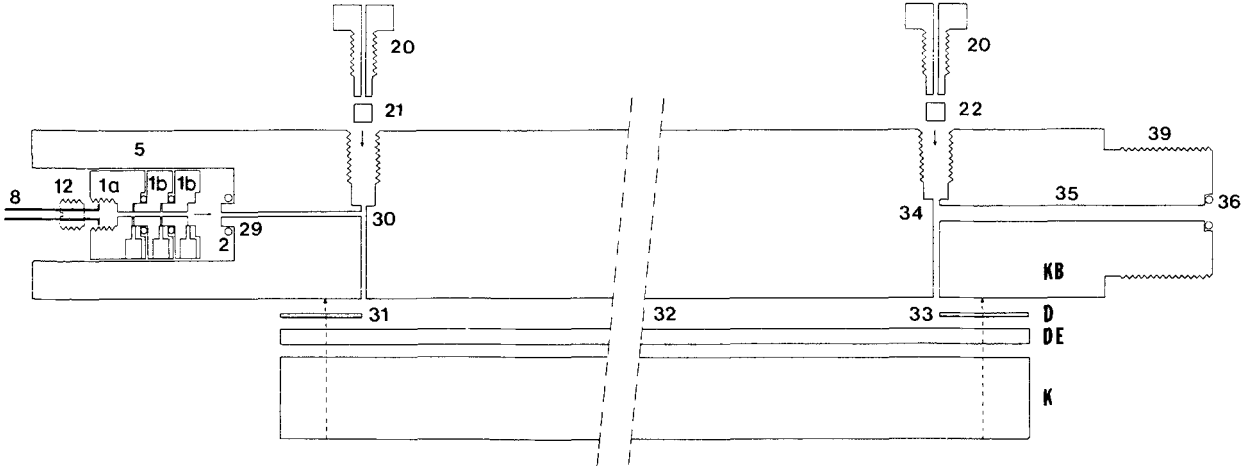

FIG. 2. Cross section and exploded assembly of the separation cell which consists of a glass plate (DE) with the detection electrodes, a Plexiglas block (KB), a silicone rubber gasket (D), and a slab of aluminum (K). Denoted parts: 1a, 1b) polyethylene terephthalate sections of inlet valve block; 1d) cylindrical projections of valve sections; 2) silicone O-ring; 4) PVC screw with center hole; 5) Plexiglass shell; 8) capillary to electrode vessel with displacing electrolyte; 9) connectors with screw (9b), flanged Teflon tube (9a) and silicone tube piece (9c); 10) holder for screw (4) and stop for expansion of the slits; 11) Plexiglass disk for pressure transfer; 12) screw holding capillary (8); 13) silicone O-ring; 15) threaded holes for external connections; 16) threaded hole for mounting of valve system; 16a) metal screw to keep holder (10) in exact position; 17) needle guide of sample inlet port; 18) silicone septum; 19) threaded cap with center hole for inlet port; 20) nylon screw with center hole; 21, 22) silicone septum; 23) mounting screws; 24) screw holes; 25) sealing edge; 26) attachment port for third electrode vessel (option); 27) screw holes for cell attachment; 28) threaded holes; 29–30–31) sensorless precolumn; 31–32–33) rectangular separation/detection trough; 33–34–35) capillary to electrode vessel with leading electrolyte; 36) silicone O-ring.

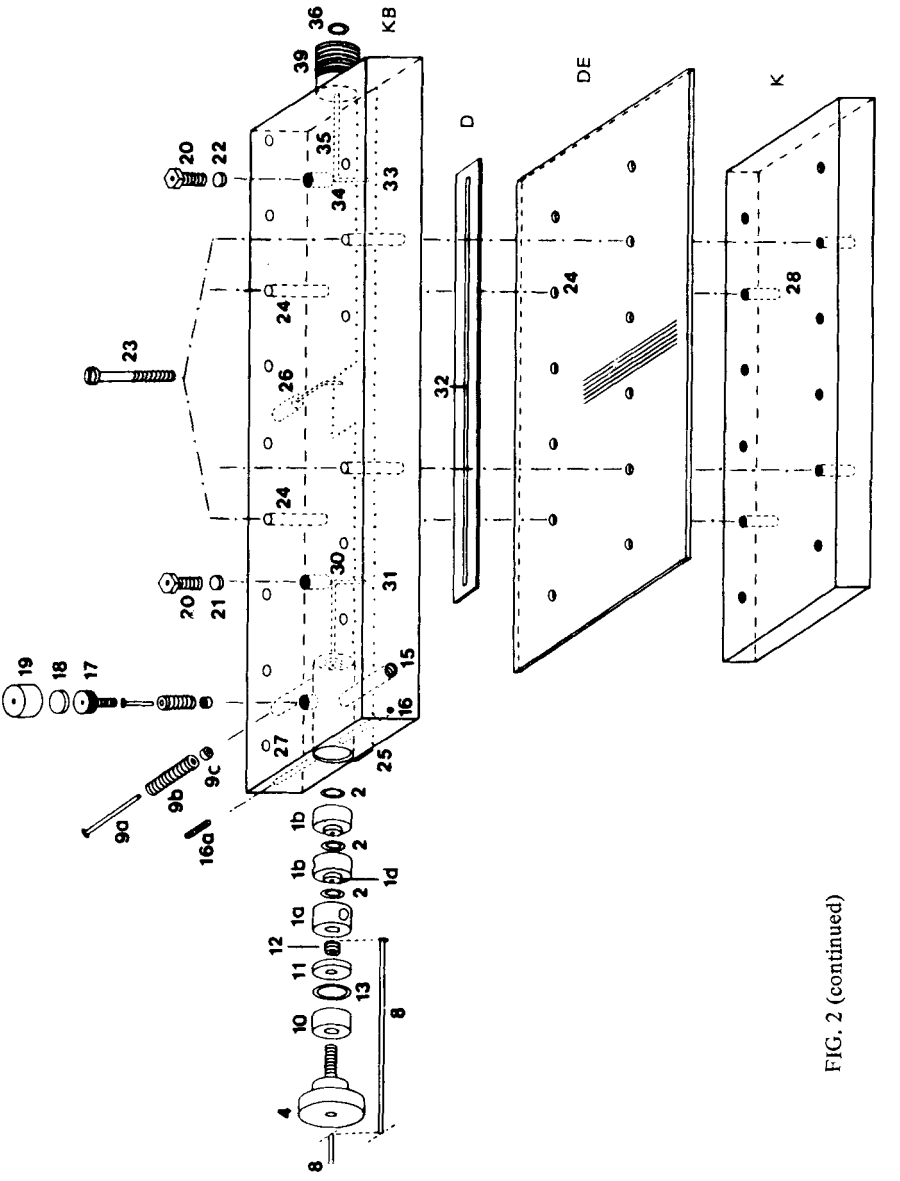

FIG. 2 (continued)

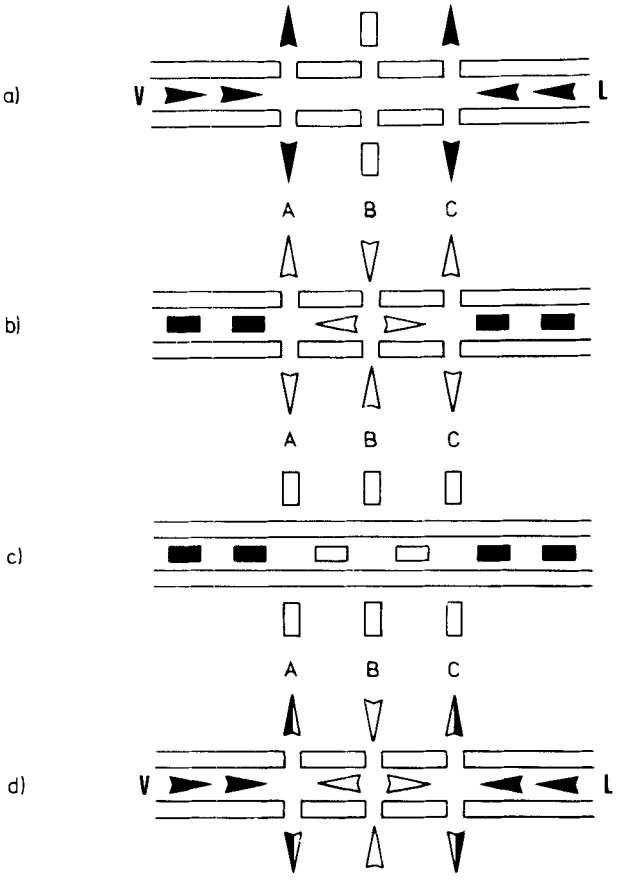

FIG. 3. Operation of sample inlet system with a constant sample volume provided by three slits (A, B, C) in the capillary. a) Simultaneous filling of the trough with leading (L) and terminating (V) electrolyte by means of 2-channel peristaltic pump. The solutions leave the capillary through slits A and C. Slit B is connected to the sample injection port. b) Injection of the sample in excess through slit B. c) Initial pattern of boundaries after closing the slits. The sample volume is enclosed between slits A and C. d) Filling procedure where sample and electrode solutions are introduced simultaneously by a 3-channel peristaltic pump.

creation of electrode patterns for liquid crystal displays. Our detection electrodes reside on the cooled glass plate which forms the lower wall of the rectangular separation capillary. We designed a unique pattern, consisting of 256 equidistant sensors (*5, 6*). They are spread over 10 cm within the separation though and perpendicular to the current flow. Electrodes are chemically photoetched on the supporting glass plate from a vapor-

deposited thin layer of a conductor. Each sensor has a width of 60 μm, a height of about 0.1 μm, and are spread 340 μm apart. We investigated Au, SnO_2, and In_2O_3/SnO_2 (80/20%) as conductor materials. SnO_2 electrodes were found to be the most suitable.

Since the potential difference between first and last sensor of the array may be as high as 15,000 V, there is no simple way of connecting each measuring channel simultaneously to a recording unit. Therefore, the electrode array is scanned mechanically at its outer edge, which is enlarged. The scanner consists of two graphite brushes (medium hard pencils) which are moved from one pair to the next pair by a stepper motor device controlled by a microprocessor (see Fig. 1). The measured potential gradient between adjacent electrodes is recorded and stored in the computer memory of a Heathkit H8 computer. We can either read data of a single pair of electrodes as a function of time (single channel run) or can scan over the whole of the detection array and get the data of each channel almost simultaneously (multichannel run). With the former operational mode, information about stable zone patterns is obtained by comparing the detected electropherograms from at least three different locations. Using the scan mode allows the detailed asymptotic approach to the steady isotachophoretic state to be followed in a completely automatic fashion. As soon as the criterion for stability is fulfilled, the microcomputer takes several scans over the total component spectrum to ensure a specified precision of zone length. All control functions, data treatment, and printout of results (field strength, length of zones with standard error, zone boundary width, and shape factor) are handled by the computer (*15, 16*).

RESULTS

We investigated the separation of maleic and phosphoric acid in the operational system listed in Table 1. The anolyte consists of a diluted solution of HCl where Cl^- represent the leading component and H_3O^+ the counterconstituent. The terminator contains lactate as anionic component, thereby forming a displacing zone of lactic acid. Using this operational system, moving pH gradients are formed due to the nonbuffering behavior of the countercomponent H_3O^+ (*1, 5, 6, 11*). In a buffer-free system the sample components usually appear in the order of increasing pK_a values. Therefore maleic acid ($pK_a = 1.91$) forms its zone in front of phosphoric acid ($pK_a = 2.12$).

The pherograms of Fig. 4 present transient and steady-state zone structures of an ITP analysis with the 2 sample components. These data are

TABLE 1
Experimental Conditions

Leading electrolyte	2.5 m*M* Hydrochloric acid
Terminating electrolyte	10.0 m*M* Na-lactate
Countercomponent	H_3O^+
Solvent	Water
Additive to leading electrolyte	0.05% Polyvinyl alcohol[a]
Driving current	200 μA
Temperature	Ambient
Separation trough	Width: 1 mm
	Height: 0.4 mm
	Length: 22.4 cm
Detection electrodes	Width: 0.06 mm
	Interval: 0.34 mm
	Number: 256
First detector at	12.4 cm
Last detector at	22.4 cm

[a]The addition of polyvinyl alcohol (Mowiol 8-88, Hoechst, Frankfurt G.F.R.) was found to minimize electroosmosis in the column and chemical reactions at the sensing electrodes.

recorded at the indicated detection channels as functions of time (single channel runs), the lower trace being the detected potential gradient and the upper the first derivative of the measured signal. When the zone structure moves across detector channel 1, four sudden field changes are recorded which indicate the existence of three homogeneous zones at this time. To check whether the second one is a mixed zone composed of maleic and phosphoric acid (detected transient state according to Fig. 1 of Ref. *8*), the mechanical scanner is moved to another location. In channel 122 the expected two-zone structure is monitored, maleic acid moving ahead of phosphoric acid. To prove that this represents steady state, the same structure has to be detected once again further in the separation trough. This was performed at detector location 240. Therefore we can conclude that the separation of the injected sample (8.51 nmol maleic and 8.79 nmol phosphoric acid) was completed between channels 1 and 122. In another experiment with the same sample we measured the potential gradient at channel 48 (Fig. 4b). Here a mixed zone smaller than that at detector location 1 is observed. This demonstrates that the length of this transient zone is decreasing with both time and location. For this particular example the two-zone structure is first monitored in channel 55 (Fig. 4c). From this point on the steady-state structure is fully established. It moves further toward the anode as long as the driving current is maintained.

The data for this pair of sample components are listed in Table 2. The

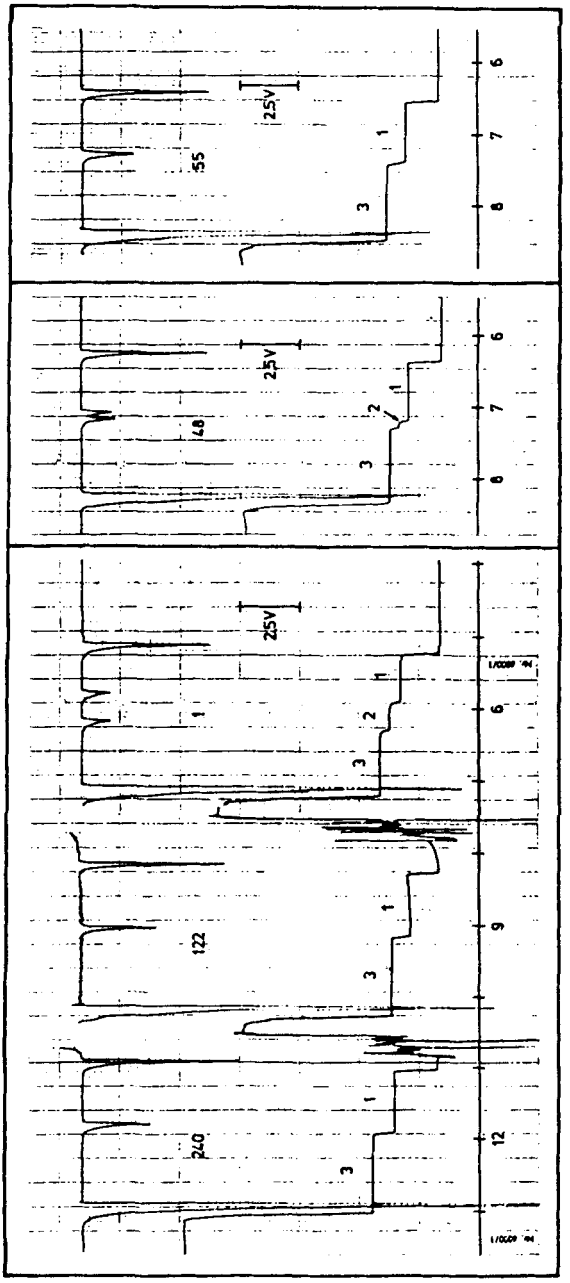

FIG. 4. The separation of two components as measured at different locations of the separation trough. The lower trace is the detected potential gradient whereas the upper is the first derivative of the measured signal. Each sudden change in the signal represents a steady-state boundary moving across the sensor. Experimental conditions: electrolyte system of Table 1; current: 200 μA; temperature: ambient; sample solution: 1.22 m*M* maleic acid, 1.26 m*M* KH_2PO_4; sample volume: 7 μL; detection channels: 1, 122, 240 (Fig. 4a), 48 (Fig. 4b), and 55 (Fig. 4c); denoted zones: 1) maleic acid, 2) mixed zone, 3) phosphoric acid.

TABLE 2
Characteristics of the Maleic/Phosphoric Acid Separation under the Experimental Conditions of Table 1. Separated Amounts are 8.51 nmol Maleic and 8.79 nmol Phosphoric Acid Respectively

a) Data Obtained from Single Channel Pherograms of Fig. 4

Detection channels	1	48	Differences, 47
Detection time of 1st boundary (s)	313.2	381.8	68.6
Detection time of 2nd boundary (s)	354.0	432.0	78.0
Detection time of 3rd boundary (s)	377.0	437.4	60.4
Detection time of steady-state zones (channels 55, 122, 240):			
Maleic acid 53.0 s			
Phosphoric acid 66.8 s			
Separation time 444 s			

b) Calculated Quantities from Experimental Data

Separated amount of maleic acid between detection channels 1 and 48	1.51 nmol	
Velocity of 1st boundary	$v_1 = 27.41 \times 10^{-3}$ cm/s	
Velocity of 2nd boundary	$v_2 = 24.10 \times 10^{-3}$ cm/s	
Separation velocity	$v = 19.36$ pmol/s	
Steady-state zone lengths within the column:	Maleic acid	1.452 cm
	Phosphoric acid	1.831 cm

c) Comparison of Experimental and Theoretical Quantities

	Experimental	Theoretical[a]
Transference number	—	10.22×10^{-2}
Separation efficiency	9.339×10^{-3}	9.648×10^{-3}
Separation parameter	10.95	10.60
Separation rate (nmol/A · s)	96.80	99.99
Separation time (s)	439.6[b]	425.5
Separation distance (cm)	15.90	15.38

[a]Based on Eqs. (2) and (9)–(12) of Ref. *8* and calculated with the following coefficients (*17*): mobilities are 37.60×10^{-9} for H_3O^+, 4.28×10^{-9} for maleinate, 3.64×10^{-9} $cm^2mol/V \cdot A \cdot s^2$ for $H_2PO_4^-$; ratio of charged species in mixed zone: $\phi = 1.0$; a (maleic acid) = 0.9, a (phosphoric acid) = 0.86.

[b]A separation time of 438.7 s is obtained with Eq. (2).

velocities of moving boundaries can be determined by comparing single channel pherograms from different locations. For that purpose the current density has to be constant. Evaluating the length decrease of the mixed zone as a function of sensor location and comparing the result obtained with the steady-state zone length allows the calculation of the separation rate, v_{sep} (mol/s). A comparative value can be given in a current independent form by

$$v'_{sep} = v_{sep}/i \qquad \text{(mol/C)} \tag{1}$$

where i is the current (A). This is the separation efficiency divided by the Faraday constant. It allows the determination of the efficiency from experimental data. By knowing the mobilities of the species and therefore the transference number, the value of the separation parameter is also obtained (*8*).

The separation time, t_{sep}, can be predicted if mobility and dissociation coefficients, as well as the ratio of the charged species in the mixed zone, are known (*8*). From the experimental results however, t_{sep} is also determinable with the velocities of the first and second boundaries of the transient zone structure, v_1 and v_2, together with the steady-state zone length of maleic acid, l_A:

$$t_{sep} = l_A/(v_1 - v_2) \qquad \text{(s)} \tag{2}$$

From single channel detection measurements, steady-state zone lengths are obtained by the time interval at which the steady-state zone moves across the sensor multiplied by the velocity of the zone structure.

The amount of maleic acid separated from the given mixture with phosphoric acid is a linear function of the location in the trough (see Eqs. 12 and 13 in Ref. *8*). This can easily be proven with the array detector. Figure 5 shows a graph representing the linear relationship between the zone length of maleic acid and the detector position (solid line). Using this graph for a given pair of sample components and the steady-state zone length permits the determination of the separation distance. In addition, it allows the calculation of the largest sample amount which can be separated before the last detector. Under the given conditions, the separation capacity was found to be 14.08 nmol maleic acid.

This maximum sample load can be enhanced by using a leading electrolyte cascade. For that purpose a higher leading electrolyte concentration is introduced in the sensorless precolumn. The zones are first adjusted to the ω value of the higher leader concentration, followed by a dilution across a stationary boundary at the location of the preestablished

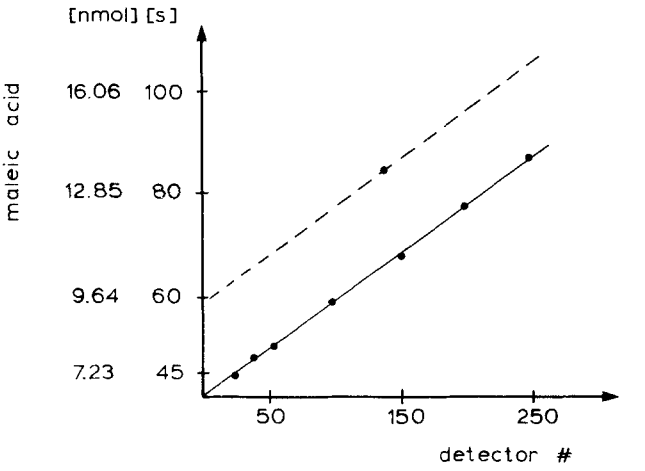

FIG. 5. The amount of maleic acid which can be separated from phosphoric acid as a function of the location in the column. The position in the capillary is expressed by the location of the array detector. The solid line represents a linear least-square fit from data based on the experimental conditions of Table 1. The slope of the linear relationship comprises the separation rate. The intercept value determines the capacity of the preseparation column and the value for detection channel 255, the separation capacity of the column with a uniform leading electrolyte. The dotted line shows the relationship under the condition of a leading electrolyte cascade with an additional amount of 75 nmol Cl^- (30 μL of 5 m*M* HCl) in the sensorless precolumn.

ω gradient. The pherograms shown in Fig. 6 represent a typical result of this effect. Here the separation of 25.53 nmol maleic and 26.37 nmol phosphoric acid was investigated, which is a three-fold increase of the sample load compared to the experiments of Fig. 4. This is beyond the separation capacity defined by the 2.5 m*M* HCl solution and the trough. Without an additional amount of the leading component, a rather long mixed zone (zone 2 of Fig. 6a) is detected at channel 140. This zone is considerably smaller at the same location when about 30 μL of 5 m*M* HCl is used as cascade electrolyte (Fig. 6b). Working under such conditions increases the separation capacity by a factor of about 1.4. This results in a parallel shift of the linear relationship between separable amount and location in the capillary, which is shown by the dashed line in Fig. 5. By using about 30 μL of a 10 m*M* HCl solution in the precolumn, the separation of the sample is completed before the zone structure moves across detector 140 (Fig. 6c). Here the total separable amount is about twice that obtained without cascade. Note that all three zone structures have the same total length. This is in agreement with the theoretical prediction.

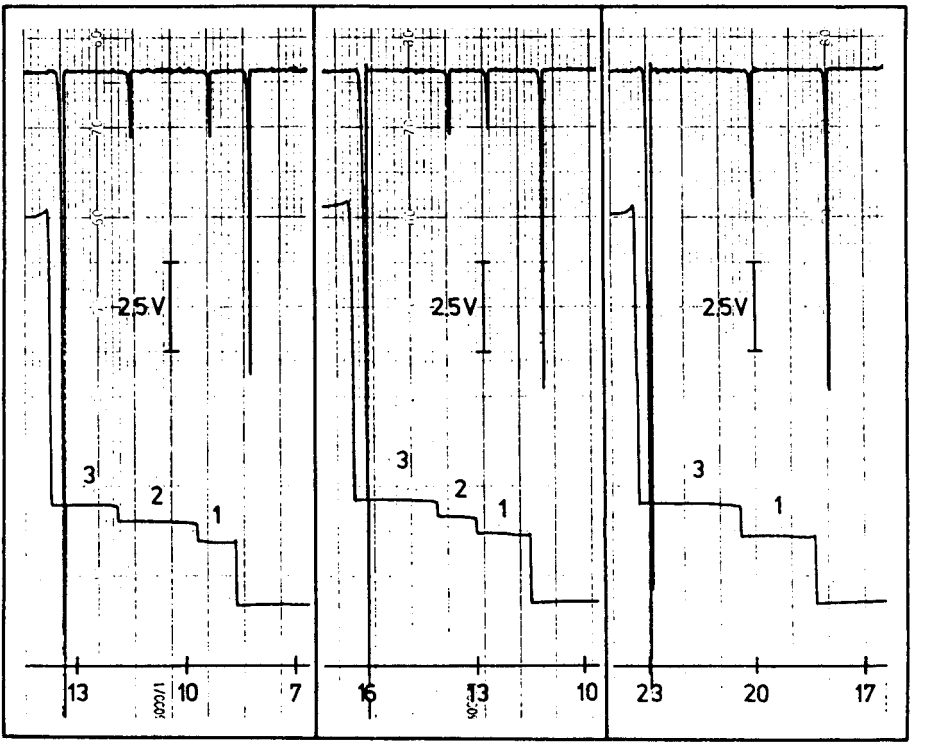

FIG. 6. Electropherograms showing the influence of a leading electrolyte cascade on the separation of maleic and phosphoric acid. The sampled amount of the two components is increased threefold compared to the experiments presented in Fig. 4. All experimental conditions listed in Table 1 are equally effective except that Runs b) and c) are performed with about 30 μL 5 m*M* and 10 m*M*, respectively, of HCl in the sensorless preseparation column. Denoted zones: 1) maleic acid, 2) mixed zone composed of maleic and phosphoric acid, 3) phosphoric acid.

DISCUSSION

The introduction of an array detector along an isotachophoretic column permits the monitoring of the attainment of the steady-state zone pattern in a straighforward fashion. In our apparatus we measure the potential gradient which is the most general physical property characterizing the separand pattern. It constitutes the first approach to automated analytical ITP where simultaneous detection of all zones is possible. This cannot be achieved in an instrument with just one detector at the end of the separation

trough. The separation of two components in a given electrolyte system is associated with the properties of the leading electrolyte which determine the normalization of the separand pattern. It can be fully predicted if mobilities and equilibrium constants are known (*8*). The availability of reliable mobility data is limited to a rather small number of components (*17*). Therefore, when a crude mixture or unknown sample is analyzed, the separation has to be followed by experimental means.

The experiments shown in this article demonstrate the capability of our device in detecting transient and steady-state zone structures of isotachophoretic separations. Single channel detection at different locations of the column illustrate the separation of two components as well as the behavior of the steady state. In addition, the effect of a leading electrolyte cascade on the separation is shown. The experiments performed demonstrate this chemical method for enhancement of the separation capacity without changing the geometry of the column. In our apparatus a twofold increase of the maximum sample load is easily obtained. The results presented agree nicely with the theoretical predictions obtained by a model based on electromigration only. It should be emphasized that this theoretical treatment of the separation process was developed for monovalent components only (*8*). Both sample components, however, are polyvalent constituents with differences between first and second pK_a values > 4. Thus, under the acidic separation conditions (pH(leader) = 2.60), they fulfill the requirement of being monovalent. The calculated pH values are 2.89 and 2.95 for the separated maleic acid and phosphoric acid zones, respectively.

An on-line evaluation of data, i.e., the comparison of consecutive scans during the experiment, is currently under investigation (*16*). This provides the last step necessary for the completion of our new concept for automation (*5*) of analytical ITP. The data from the 255 detection channels are ideally suited for computer treatment (*15*): The source noise is small, the general property measurements are integrals, which means that no integration is required for quantitation, and pattern recognition is limited to acceptance or refusal of a zone boundary. Compared to single channel detection at the end of the separation column, the duration of an analysis is shortened and the precision of zone length determinations is increased by multiple, independent measurements. Furthermore, proper analytical self-testing and elaborate data analysis are performed automatically, unnoticed by the user. At the end a written report is in hand before one conventional single channel run is even finished. Calibration runs provide necessary data for automated identification and quantitation of sample components.

We believe that our apparatus is not only an important tool for the automation of ITP, but for the better understanding of all fundamental

electrophoretic processes as well. The multichannel detector permits following the moving boundaries which represent electric field changes in moving boundary electrophoresis (MBE) (*18*), zone electrophoresis (ZE) (*18, 19*), and isoelectric focusing (IEF). This device will be used for validation studies of computer predictions in electrophoresis (*20*).

Acknowledgments

The authors would like to express their gratitude to Drs M. Bier and R. A. Mosher for helpful discussions. This work was sponsored by the "Kommission zur Foerderung der wissenschaftlichen Forschung," Bern, Grant No. 1074 and by CIBA-GEIGY AG, Basel, Switzerland.

REFERENCES

1. E. Schumacher and T. Studer, *Helv. Chim. Acta, 47*, 957 (1964).
2. F. M. Everaerts, J. L. Beckers, and T. P. E. M. Verheggen, *Isotachophoresis*, in *Journal of Chromatography Library*, Vol. 6, Elsevier, Amsterdam, 1976.
3. P. Boček, *Top. Curr. Chem., 95*, 131 (1981).
4. M. Bier and T. T. Allgyer, in *Electrokinetic Separation Methods* (P. G. Righetti, C. J. van Oss, and P. J. Vanderhoff, eds.), Elsevier, Amsterdam, 1979, p. 443.
5. E. Schumacher, W. Thormann, and D. Arn, in *Analytical Isotachophoresis* (F. M. Everaerts, ed.), Elsevier, Amsterdam, 1981, p. 33.
6. W. Thormann, PhD Thesis, University of Bern, Switzerland, 1981.
7. W. Thormann, *Swiss Med., 3*(12), 46 (1981).
8. W. Thormann, *Sep. Sci. Technol., 19*, 455 (1984), and references cited therein.
9. P. Boček, M. Deml, and J. Janák, *J. Chromatogr., 106*, 283 (1975).
10. S. Hjertén, *Protides Biol. Fluids, Proc. Colloq., 22*, 669 (1975); S. Hjertén, L. G. Oefverstedt, and G. J. Johansson, *J. Chromatogr., 194*, 1 (1980).
11. P. Ryser, PhD Thesis, University of Bern, Switzerland, 1976.
12. P. Boček, M. Deml, and J. Janák, *J. Chromatogr., 156*, 323 (1978).
13. F. M. Everaerts, T. P. E. M. Verheggen, and F. E. P. Mikkers, *Ibid., 169*, 21 (1979).
14. Z. Ryšlavý, P. Boček, M. Deml, and J. Janák, *Ibid., 147*, 369 (1978).
15. E. Schumacher, D. Arn, and W. Thormann, *Electrophoresis, 4*, 390 (1983).
16. D. Arn, PhD Dissertation, University of Bern, Switzerland, In Preparation.
17. T. Hirokawa, M. Nishino, N. Aoki, Y. Kiso, Y. Sawamoto, T. Yagi, and J. Akiyama, *J. Chromatogr., 271*, D1 (1983).
18. W. Thormann, D. Arn, and E. Schumacher, in *Electrophoresis '83* (H. Hirai, ed.), Walter de Gruyter, Berlin, 1984, p. 109.
19. W. Thormann, *Electrophoresis, 4*, 383 (1983).
20. M. Bier, O. A. Palusinski, R. A. Mosher, and D. A. Saville, *Science, 219*, 1281 (1983).

Received by editor March 19, 1984
Revised April 17, 1984